

# Magnetic freezing and spin frustration in the triangular lattice magnets $\text{GdI}_2\text{H}_x$ ( $0 \leq x < 1$ )

Mikhail Ryazanov, Arndt Simon, and Reinhard K. Kremer

*Max-Planck Institut für Festkörperforschung, Heisenbergstrasse 1, D-70569 Stuttgart, Germany*

(Received 6 July 2007; revised manuscript received 20 February 2008; published 17 March 2008)

The magnetic properties of hydrogen-doped  $\text{GdI}_2\text{H}_x$  ( $0 \leq x < 1$ ) have been studied by dc and ac magnetic susceptibility and field dependent magnetization measurements. The susceptibility data of  $\text{GdI}_2$  indicate strong ferromagnetic correlations which develop below 320 K and lead to long-range magnetic ordering at  $T_C \approx 280$  K. Hydrogen insertion into  $\text{GdI}_2$  introduces antiferromagnetic interactions, and the susceptibility shows a diminishing signature of a three-dimensional ferromagnetic transition. Furthermore, the low-temperature susceptibilities of  $\text{GdI}_2\text{H}_x$  ( $x=0.19, 0.26$ ) exhibit frequency dependencies which are attributed to freezing of ferromagnetic clusters.  $\text{GdI}_2\text{H}_{0.42}$  exhibits spin-glass-like behavior, confirmed by frequency-dependent peaks in the real part of the ac susceptibility and a magnetic hysteresis loop below freezing temperature  $T_f \approx 24$  K. Spin relaxation phenomena observed are ascribed to spin frustration effects, caused by competing ferromagnetic and antiferromagnetic interactions.

DOI: 10.1103/PhysRevB.77.104423

PACS number(s): 75.50.Lk, 75.30.Cr

## I. INTRODUCTION

In recent years, gadolinium di-iodide ( $\text{GdI}_2$ ), formally containing Gd in the unusual +2 oxidation state, was investigated in detail with regard to its electrical transport and magnetic properties.<sup>1–5</sup>  $\text{GdI}_2$  is a layered metallic compound which orders ferromagnetically near room temperature and shows a large negative magnetoresistance (MR) of  $\approx 70\%$  at 300 K in a 70 kOe magnetic field. These remarkable properties are closely related to the structural and electronic features of the system.  $\text{GdI}_2$  crystallizes in the hexagonal  $2H\text{-MoS}_2$  structure type and comprises triangular layers of metal atoms sandwiched by close-packed layers of iodine atoms (Fig. 1). Such  $\text{GdI}_2$  slabs are interconnected along the  $c$  axis via van der Waals contacts, thus indicating a pronounced structural anisotropy. The metal atoms have a  $4f^7 5d^1$  electronic configuration. In addition to the half-filled  $4f$  magnetic core of the  $\text{Gd}^{3+}$  ions, an extra electron is delocalized in the  $\text{Gd } 5d$  conduction band and is involved in Gd-Gd bonding.

The colossal magnetoresistance (CMR) in  $\text{GdI}_2$  has been interpreted quantitatively in terms of spin-disorder scattering of the  $5d$  conduction electrons by the localized  $4f$  electrons coupled via  $d$ - $f$  exchange.<sup>5,6</sup> In fact, this scenario has been supported by recent electron spin resonance experiments which indicate a correlation between spin and charge degrees of freedom.<sup>7</sup> From spin-polarized band structure calculations,<sup>3</sup> it has been proposed that the CMR in  $\text{GdI}_2$  can be further increased by hole doping of the system, e.g., with hydrogen. Indeed,  $\text{GdI}_2\text{H}_x$  samples with  $x=0.2\text{--}0.3$  exhibit an enhanced negative MR as large as 95% at 150 K and  $H=70$  kOe.<sup>8</sup> Furthermore, insertion of hydrogen into  $\text{GdI}_2$  leads to significant changes in both the electrical and magnetic properties.<sup>2,9</sup>  $\text{GdI}_2\text{H}_x$  shows thermally activated electrical conduction, and dc magnetic susceptibility measurements reveal a rich magnetic phase diagram as a function of the hydrogen content.<sup>9</sup> The system moves from ferromagnetism to a spin-glass-like magnetic state at a critical hydrogen content of  $x \approx 1/3$ , while hydrogen-rich  $\text{GdI}_2\text{H}_x$  phases ( $x > 0.7$ ) are paramagnetic down to 2 K. In addition, the fer-

romagnetic samples exhibit thermal hysteresis of the zero-field-cooled and field-cooled dc susceptibilities at low temperatures, which is a common signature of systems with a spin-frozen state or compounds exhibiting narrow-domain-wall ferromagnetism. However, from dc magnetic measurements, one cannot clearly identify the low-temperature magnetic state of the system.

Here, we report measurements of the ac magnetic susceptibility and isothermal magnetization of  $\text{GdI}_2$  and of a series of  $\text{GdI}_2\text{H}_x$  samples covering the composition range  $0 < x < 1$ . The ferromagnetic compounds  $\text{GdI}_2\text{H}_{0.19}$  and  $\text{GdI}_2\text{H}_{0.26}$  show anomalous magnetic relaxation phenomena, whereas typical characteristics of a spin glass are observed for  $\text{GdI}_2\text{H}_{0.42}$ .

## II. EXPERIMENT

The binary compound  $\text{GdI}_2$  was synthesized by solid state reaction of sublimed  $\text{GdI}_3$  with Gd filings (99.99%; Johnson Matthey, Karlsruhe) at 820 °C for 30 days in tantalum tubes filled with argon and closed by arc welding. Hydrogenation up to  $x=0.97$  was carried out in a Sieverts-type apparatus<sup>10</sup> by slowly heating  $\text{GdI}_2$  in a closed system under 1 atm  $\text{H}_2$  (99.999%; Messer-Griesheim).  $\text{GdI}_2\text{H}_x$  samples ( $x < 0.97$ )

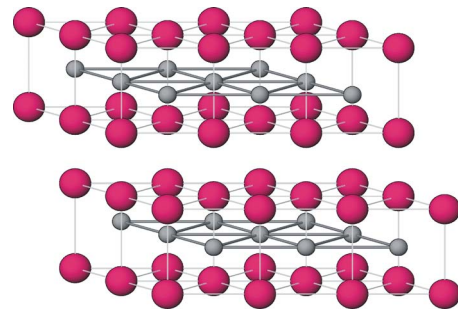


FIG. 1. (Color online) Perspective view of the hexagonal crystal structure of  $\text{GdI}_2$ . Gd and I atoms are depicted with increasing size. The thick lines symbolize the metal-metal bonds.

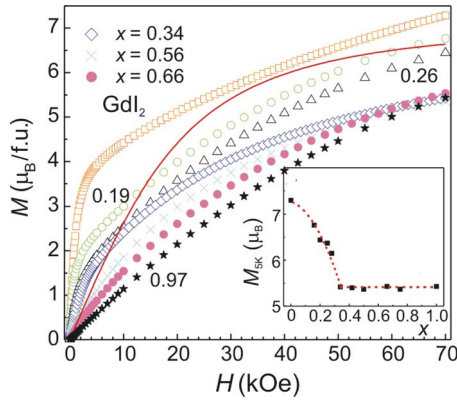


FIG. 2. (Color online) Magnetic moment (per f.u.) vs applied field for  $\text{GdI}_2\text{H}_x$  at 5 K. The solid line corresponds to the Brillouin function for a system of isolated  $S=7/2$  moments. The inset displays the saturation magnetic moments  $M$  (5 K, 70 kOe) as a function of  $x$ .

were prepared by heating pressed pellets of appropriate quantities of  $\text{GdI}_2$  and  $\text{GdI}_2\text{H}_{0.97}$  at  $650^\circ\text{C}$  for 2–3 days in Mo ampoules jacketed by Ar-filled silica tubes.

The hydrogen content  $x$  in  $\text{GdI}_2\text{H}_x$  was determined by chemical analysis via combustion and coulometric titration of the generated  $\text{H}_2\text{O}$  (Karl Fischer method<sup>11</sup>). The error in determining  $x$  was  $\Delta x = \pm 0.03$ . A more detailed description of the sample preparation and the structural characterization may be found elsewhere.<sup>9</sup>

Since the studied compounds are very sensitive to air and moisture, all handling of the samples was performed under inert atmosphere employing the Schlenk technique (or glovebox,  $\text{H}_2\text{O}$  and  $\text{O}_2$  below  $\approx 0.2$  and  $\approx 0.8$  ppm, respectively).

The ac magnetic susceptibility data were collected in a commercial physical properties measurement system (PPMS, Quantum Design) between 2 and 350 K in a 1 Oe ac magnetic field and measurement frequencies varying from 10 to  $10^4$  Hz. The powder samples were pressed into cylindrical pellets (diameter of 3 mm, thickness of  $\approx 0.5$  mm) and sealed in quartz glass ampoules under 1 atm He exchange gas to provide sufficient thermal contact. dc magnetizations ( $B \perp$  disk) were measured at 5 K in magnetic fields up to 70 kOe using a superconducting quantum interference device magnetometer (MPMS, Quantum Design). To measure the magnetic hysteresis loops, the samples were first cooled in zero field to the set temperature, and then the applied field was subsequently cycled between  $\pm 70$  kOe.

### III. RESULTS

#### A. dc magnetizations

In order to get a first insight into the nature of the low-temperature magnetic state, we performed dc magnetization measurements on  $\text{GdI}_2\text{H}_x$  ( $0 \leq x < 1$ ) as a function of applied field at temperatures well below the magnetic transition temperatures. Figure 2 shows the magnetization curves  $M(H)$  at 5 K for a number of samples with various hydrogen contents. The Brillouin function for free  $\text{Gd}^{3+}$  moments ( $S$

$= 7/2$ ) is also shown. For  $\text{GdI}_2$ , the magnetization grows very rapidly at low fields, indicating spontaneous ordering. However, the magnetization does not level off at higher fields but rather increases almost linearly with the applied field, reaching  $7\mu_B$  at  $H \approx 60$  kOe, expected for the spin-only  $4f^7$  configuration. The magnetization of our present  $\text{GdI}_2$  sample does not show the rapid increase as has been reported by Felser *et al.* before.<sup>3</sup> There, saturation has been observed essentially above 20–30 kG with saturation magnetizations of  $M_{\text{sat}} \approx 7.3\mu_B$ , with the excess magnetization corresponding to  $\approx 0.3\mu_B$  per Gd atom arising from a strong polarization of the  $5d$  conduction electrons. The difference in the two magnetization curves may be due to crystalline anisotropy. In the measurement on the loosely filled in polycrystalline sample used in Ref. 3, the crystallites may have easily reoriented with increasing magnetic field, while in our experiments carried out on pressed pellets, this is not possible and one has to overcome the magnetocrystalline anisotropy to saturate the sample.

Insertion of hydrogen into  $\text{GdI}_2$  leads to a lowering of the saturation magnetization compared with that of the binary compound. Similar as in  $\text{GdI}_2$ , the magnetizations of  $\text{GdI}_2\text{H}_x$  samples with low hydrogen content ( $x < 0.4$ ) show a steep increase in low magnetic fields, well exceeding the calculated values for a paramagnetic system. However,  $M$  falls below the Brillouin function expected for free  $\text{Gd}^{3+}$  moments upon increasing  $H$  above  $\approx 10$  kOe. This behavior indicates competition of ferromagnetic and antiferromagnetic interactions. Kasten *et al.* had already inferred some canting of the moments in  $\text{GdI}_2$  due to the presence of antiferromagnetic correlations.<sup>1</sup> For the hydrogen-rich samples with  $x > 0.5$ , the magnetization data lie below the Brillouin function already in low fields, indicating that the antiferromagnetic component enhances with increasing  $x$ . Another remarkable feature is the variation of the magnetic moments  $M$  (5 K, 70 kOe) of  $\text{GdI}_2\text{H}_x$  as a function of the hydrogen content. As shown in the inset of Fig. 2, these values decrease significantly from  $7.3\mu_B$  to  $5.4\mu_B$  when  $x$  approaches a critical concentration of  $\approx 0.33$ , whereas the moment remains almost unchanged for higher  $x$ .

The magnetic data  $M(H)$  collected on zero-field-cooled  $\text{GdI}_2$  and  $\text{GdI}_2\text{H}_x$  ( $x=0.26$  and  $0.42$ ) samples upon varying  $H$  between  $\pm 70$  kOe indicate irreversible behavior for all three samples. For the ferromagnetic systems  $\text{GdI}_2$  and  $\text{GdI}_2\text{H}_{0.26}$ , there is a strong irreversibility between the pristine magnetization curve and field-cycled branches at low fields (Fig. 3). Similar effects have been observed for canted spin systems and spin glasses.<sup>13,14</sup> The field-driven changes in the magnetization of  $\text{GdI}_2\text{H}_{0.42}$  result in a symmetrical hysteresis loop shown in the inset of Fig. 3, which is consistent with the expected behavior of systems with competing interactions.

#### B. ac magnetizations

Figure 4 shows the temperature dependencies of the real component  $\chi'$  of the ac magnetic susceptibilities measured for zero (dc)-field-cooled  $\text{GdI}_2$ ,  $\text{GdI}_2\text{H}_{0.19}$ ,  $\text{GdI}_2\text{H}_{0.26}$ , and  $\text{GdI}_2\text{H}_{0.42}$  samples.

In the ferromagnetic state,  $\chi'$  of  $\text{GdI}_2$  increases slightly with increasing temperature up to 250 K, followed by a

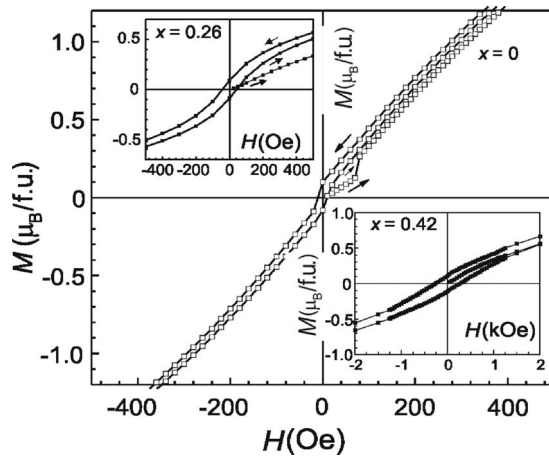


FIG. 3. Hysteresis loops for  $\text{GdI}_2$  and  $\text{GdI}_2\text{H}_x$  samples with  $x=0.26$  and  $x=0.42$  at 5 K.

sharp drop at the Curie temperature  $T_C \approx 280$  K, determined as the temperature where  $\chi'(T)$  exhibits the steepest descent. With hydrogen insertion, the transition broadens and shifts to lower temperatures. For the hydrogenated samples with  $x=0.19$  and  $0.26$ ,  $\chi'$  is characterized by a broad maximum and a shallow kink at  $\approx 100$  and  $\approx 20$  K, respectively. The kink is substantially decreased with increasing frequency, while the broad maximum decreases in magnitude ( $\approx 3\%$ ) as the frequency increases from 10 Hz to 10 kHz (not shown). For  $\text{GdI}_2\text{H}_{0.42}$ ,  $\chi'$  increases gradually with decreasing temperature down to 30 K. At lower temperatures, there is a rounded kink centered at  $\approx 24$  K. Below 5 K, a slight increase of the susceptibility appears again.

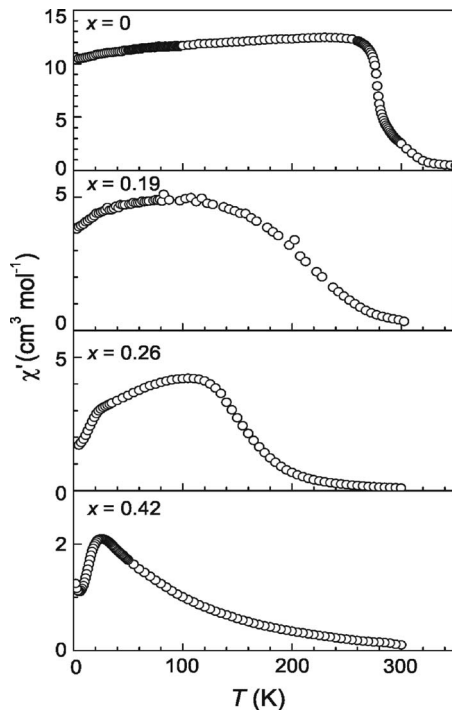


FIG. 4. Temperature dependence of the real part of the ac magnetic susceptibility  $\chi'$  (ac field=1 Oe, frequency=100 Hz) for  $\text{GdI}_2\text{H}_x$ .

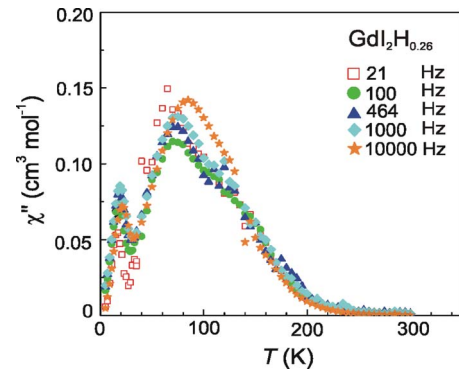


FIG. 5. (Color online) Temperature dependence of the imaginary component of the ac magnetic susceptibility of  $\text{GdI}_2\text{H}_{0.26}$  measured at various frequencies in a 1 Oe ac field.

The systematic shifts with increasing hydrogen content of  $\chi'(T)$  to low temperatures and the final narrowing into a kink for  $\text{GdI}_2\text{H}_{0.42}$  is paralleled by temperature and frequency dependences of the imaginary parts  $\chi''(T)$  of the susceptibilities.

For  $\text{GdI}_2\text{H}_{0.26}$  the imaginary part  $\chi''(T)$  also exhibits frequency-dependent anomalies (Fig. 5). At low frequencies, a nonzero  $\chi''$  develops with decreasing temperature below 200 K, which passes through a maximum centered at  $\approx 80$  K. In addition, a well-defined peak in  $\chi''(T)$  is seen at 18 K.

Figure 6 shows the temperature behavior of the real and imaginary components of the ac magnetic susceptibility for the  $\text{GdI}_2\text{H}_{0.42}$  sample.  $\chi'$  increases gradually with decreasing temperature down to 30 K. At lower temperatures, there is a

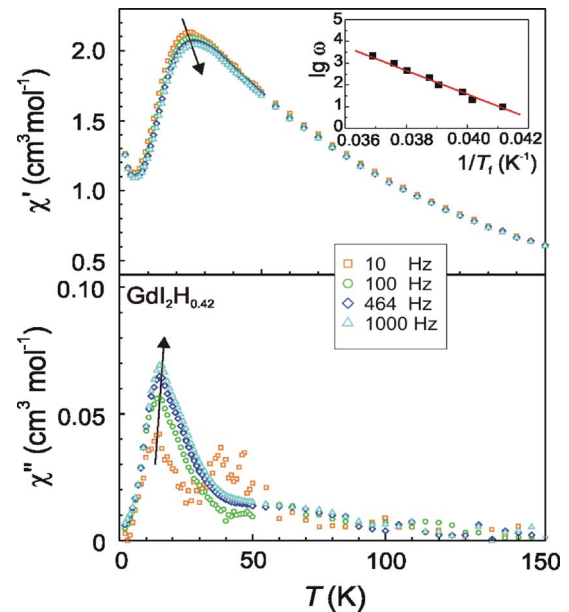


FIG. 6. (Color online) Temperature dependencies of the real ( $\chi'$ ) and imaginary ( $\chi''$ ) components of the ac magnetic susceptibility of  $\text{GdI}_2\text{H}_{0.42}$  in a 1 Oe ac field with the arrows denoting increasing frequency. The inset displays measurement frequency (logarithmic scale) vs the inverse of the freezing temperature.

rounded kink in  $\chi'$  around  $\approx 24$  K.  $\chi'$  increases below 50 K and develops a sharp cusp at  $\approx 15$  K. Both  $\chi'$  and  $\chi''$  are frequency dependent.  $\chi'$  shifts toward higher temperatures with increasing  $\omega$ , while its magnitude decreases by about 4% as the frequency increases from 10 to 1000 Hz. In contrast, the peak height and relative amplitude of the high-temperature shoulder in  $\chi''(T)$  both increase with the frequency. The observed frequency-dependent anomalies in ac susceptibility are characteristic of a spin-disordered system. The relative temperature shift of the ac magnetic susceptibility peak per decade of the frequency  $\omega$  offers a good criterion for distinguishing different kinds of disordered systems such as canonical spin glasses, cluster-glass-like materials, or superparamagnets.<sup>12</sup> The inset in Fig. 6 shows the dependence of the inverse freezing temperature  $1/T_f$  vs  $\log \omega$ , with  $T_f$  defined as the maximum in  $\chi'(T)$ . The observed linear behavior corresponds to a shift of  $\Delta T_f/T_f$  per decade in  $\omega$  of  $\approx 0.04$  which is of the same order of magnitude as the  $\Delta T_f/[T_f(\Delta \log \omega)]$  values commonly found in other insulating spin glasses and cluster glass systems.<sup>12</sup>

#### IV. DISCUSSION

The appearance of an imaginary component of the ac susceptibility reflects the energy losses occurring during the magnetization reversal in the ac magnetic field. Such effects are usually found in hard ferromagnets with nonzero coercivity or in systems developing spin freezing. For virtually soft ferromagnet  $\text{GdI}_2$  with the spin-only  $^8S_{7/2}$  ground state, a nonzero  $\chi''$  already appearing above  $T_C$  is likely due to strong short-range magnetic ordering effects. As has been found in previous studies on  $\text{GdI}_2$ ,<sup>5,9</sup> the dc susceptibility does not follow a Curie–Weiss law up to 600 K, thus suggesting the existence of correlated magnetic clusters in the paramagnetic state. We assume that the magnetic moments within a single metal atom layer correlate ferromagnetically already at about 320 K to form two dimensional ferromagnetic (fm) domains. The interlayer magnetic coupling is mainly mediated by dipolar interactions through bilayers of iodine atoms linked via weak van der Waals interactions, and they have been estimated to be approximately 30 times weaker than the intraplane exchange.<sup>5</sup> With decreasing temperature, the interlayer coupling becomes relevant; hence, a bulk magnetic transition occurs at  $T_C \approx 280$  K. On the other hand, the almost linear increase of the low-temperature magnetization at high fields (Fig. 2) implies the presence of antiferromagnetic correlations in  $\text{GdI}_2$ , which we attribute to weak antiferromagnetic second-neighbor exchange ( $J_{\text{NNN}}$ ) within the layers. For a triangular layer system, this situation would result in spin tilting away from a collinear alignment or even in a helical spin structure if  $J_{\text{NNN}}$  is sufficiently large,<sup>15</sup> thus giving rise to some degree of frustration in the magnetic lattice. The low-temperature anomalies seen in  $\chi''(T)$  are attributed to spin-reorientation effects induced by the ac magnetic field, which should be easily enabled for the Gd-based compounds with small, if any, single-ion anisotropy.

For the hydrogenated  $\text{GdI}_2\text{H}_x$  samples,  $0.19 \leq x \leq 0.42$ , frequency-dependent maxima are observed in both the real

and imaginary parts of the ac magnetic susceptibility, indicative of spin freezing at low temperatures. The latter is associated with the increasing antiferromagnetic (afm) interactions which develop with rising  $x$ . Insertion of hydrogen into the trigonal Gd layers plays a dual role on the magnetic properties of  $\text{GdI}_2\text{H}_x$ . First, it leads to localization of the conduction electrons at hydride ions such that the fm interaction weakens with increasing H content. Second, the magnetic coupling within the hydrogen-filled  $\text{Gd}_3\text{H}$  units mediated by superexchange via the  $\text{H}^-$  ions is found to be afm, in agreement with the Goodenough–Kanamori rules for nonorthogonal and half-occupied magnetic orbitals.<sup>16,17</sup> The presence of afm clusters in a fm matrix leads to a local spin frustration. This general statement can be considered in more detail for the ferromagnetic  $\text{GdI}_2\text{H}_{0.19}$  and  $\text{GdI}_2\text{H}_{0.26}$  samples. As shown in Fig. 6 for the latter composition, two frequency-dependent anomalies in  $\chi''$  are observed, which indicate different magnetic relaxations in the system. As the high-temperature anomaly rather vanishes in the composition range of the spin glasses ( $x=0.42$ ) (see Fig. 6), this broad anomaly is attributed to the dynamics of large ferromagnetic clusters with a considerable size distribution, and it involves domain wall movement. The low-temperature cusp can be associated with local spin flips in and around the antiferromagnetically coupled Gd atoms of the  $\text{Gd}_3\text{H}$  units.

When the hydrogen content exceeds the critical value  $x_{\text{crit}}=1/3$ , the long-range ferromagnetic order breaks down, and the magnetic ground state becomes fully frustrated since for  $x \geq 1/3$  and local H order within the layers, competing fm and afm interactions act on each magnetic moment.<sup>9</sup> In fact, the sample with  $x=0.42$  exhibits spin glass behavior accompanied by relaxation processes. The frequency shift of the freezing temperature  $T_f$  for this composition can be described by the Vogel–Fulcher (VF) model,  $\omega = \omega_0 \exp[-E_a/k(T_f - T_0)]$ , often used in the case of magnetically interacting clusters (micromagnetism). Here, the parameter  $T_0$  is related to intercluster interaction strengths. The VF law provides a good fit to our data with the following parameters:  $\omega_0 = 5 \times 10^{11}$  Hz,  $E_a = 244 \pm 10$  K, and  $T_0 = 14.5 \pm 0.5$  K. It is noteworthy that, in contrast to many known spin-glass-like systems in which the required randomness coupled with a magnetic frustration is caused by site disorder in the magnetic sublattices, the disorder in  $\text{GdI}_2\text{H}_x$  is introduced in the diamagnetic H atom sublattice, similar to the related system  $\text{TbBrH}_x$ .<sup>18</sup>

Further evidence of the cooperative spin-frustrated state in  $\text{GdI}_2\text{H}_x$  ( $x > x_{\text{crit}}$ ) comes from the fact that the low-temperature magnetic moment is almost identical for all samples with  $x > 1/3$ , reaching a value of  $\approx 5.4\mu_B$  at  $H = 70$  kOe (see Fig. 2 inset). It is interesting to note that, when assuming the Gd spins to be oriented parallel to the triangular layers,<sup>19</sup> the observed saturation magnetizations  $M_s(5 \text{ K}, 70 \text{ kOe})$  are close to values of  $5.2\mu_B - 5.6\mu_B$  calculated for the canted magnetic arrangements sketched in the inset of Fig. 2.<sup>20</sup>

In conclusion, we have investigated the magnetic behavior of  $\text{GdI}_2\text{H}_x$  in dc and ac magnetic fields. Measurements on  $\text{GdI}_2$  indicate the existence of strong ferromagnetic correlations which start developing at 320 K and lead to long-range

magnetic ordering at  $T_C \approx 280$  K. When inserting hydrogen into  $\text{GdI}_2$ , antiferromagnetic interactions are introduced, which result in a local spin frustration within ferromagnetic domains. Provided there is an ordering of the  $\text{H}^-$  ions due to Coulomb repulsion between them, the total spin frustration is reached at a critical composition  $\text{GdI}_2\text{H}_{0.33}$ , where the system becomes a spin glass. As expected from dc magnetic measurements,<sup>9</sup> the  $\text{GdI}_2\text{H}_{0.42}$  sample exhibits conventional spin-glass-like characteristics such as frequency-dependent peaks in  $\chi_{ac}$  and a magnetic hysteresis loop below freezing temperature  $T_f \approx 24$  K. The ferromagnetic  $\text{GdI}_2\text{H}_x$  samples ( $x=0.19$  and  $0.26$ ) exhibit two characteristic anomalies in

$\chi_{ac}(T)$ , reflecting different magnetic relaxations in the system. The broad high-temperature anomaly around 80 K is related to ferromagnetic ordering in clusters of widely varying sizes. The low-temperature cusp at around 20 K anticipates the characteristic feature of the spin glass phase. This cusp remains almost at the same temperature and its shape does not significantly change for  $0 < x < 0.42$ , in contrast to the high-temperature anomaly. The presence of both features in samples with the intermediate hydrogen content,  $0 < x < 0.33$ , indicates a magnetically inhomogeneous system with phase separation into ferromagnetic and spin glass components.

- 
- <sup>1</sup>A. Kasten, P. H. Mueller, and M. Schienle, *Solid State Commun.* **51**, 919 (1985).
- <sup>2</sup>C. Michaelis, W. Bauhofer, H. Buchkremer-Hermanns, R. K. Kremer, A. Simon, and G. J. Miller, *Z. Anorg. Allg. Chem.* **618**, 98 (1992).
- <sup>3</sup>C. Felser, K. Ahn, R. K. Kremer, R. Seshadri, and A. Simon, *J. Solid State Chem.* **147**, 19 (1999).
- <sup>4</sup>K. Ahn, C. Felser, R. Seshadri, R. K. Kremer, and A. Simon, *J. Alloys Compd.* **303-304**, 252 (2000).
- <sup>5</sup>I. Eremin, P. Thalmeier, P. Fulde, R. K. Kremer, K. Ahn, and A. Simon, *Phys. Rev. B* **64**, 064425 (2001).
- <sup>6</sup>T. Maitra, A. Taraphder, A. N. Yaresko, and P. Fulde, *Eur. Phys. J. B* **49**, 433 (2006).
- <sup>7</sup>J. Deisenhofer, H.-A. Krug von Nidda, A. Loidl, K. Ahn, R. K. Kremer, and A. Simon, *Phys. Rev. B* **69**, 104407 (2004).
- <sup>8</sup>M. Ryazanov, A. Simon, R. K. Kremer, and Hj. Mattausch, *Phys. Rev. B* **72**, 092408 (2005).
- <sup>9</sup>M. Ryazanov, A. Simon, R. K. Kremer, and Hj. Mattausch, *J. Solid State Chem.* **178**, 2339 (2005).
- <sup>10</sup>C. Michaelis, Hj. Mattausch, and A. Simon, *Z. Anorg. Allg. Chem.* **610**, 23 (1992).
- <sup>11</sup>R. Eger, Hj. Mattausch, and A. Simon, *Z. Naturforsch. B* **48**, 48 (1993).
- <sup>12</sup>J. A. Mydosh, *Spin Glasses: An Experimental Introduction* (Taylor & Francis, London, 1993).
- <sup>13</sup>R. W. Knitter, J. S. Kouvel, and H. Claus, *J. Magn. Magn. Mater.* **5**, 356 (1977).
- <sup>14</sup>P. A. Beck, *Prog. Mater. Sci.* **23**, 1 (1980).
- <sup>15</sup>T. Sakakibara, *J. Phys. Soc. Jpn.* **53**, 3607 (1984).
- <sup>16</sup>J. B. Goodenough, *Phys. Rev.* **100**, 564 (1955).
- <sup>17</sup>J. Kanamori, *J. Phys. Chem. Solids* **10**, 87 (1959).
- <sup>18</sup>R. K. Kremer, W. Bauhofer, Hj. Mattausch, W. Brill, and A. Simon, *Solid State Commun.* **73**, 281 (1990).
- <sup>19</sup>Cited from Ref. 1.
- <sup>20</sup>M. Ryazanov, Ph.D. thesis, Universität Stuttgart, 2004.